

1<sup>st</sup> CIRP Conference on Surface Integrity (CSI)

## The effects of Cryogenic Cooling on Surface Integrity in Hard Machining

D. Umbrello<sup>a,b\*</sup>, Z. Pu<sup>b</sup>, S. Caruso<sup>a</sup>, J.C. Outeiro<sup>c,d</sup>,  
A.D. Jayal<sup>b</sup>, O.W. Dillon Jr.<sup>b</sup>, I.S. Jawahir<sup>b</sup>

<sup>a</sup>University of Calabria, Department of Mechanical Engineering, Rende (CS), 87036, Italy

<sup>b</sup>University of Kentucky, Institute for Sustainable Manufacturing (ISM), Lexington, KY 40506, USA

<sup>c</sup>Catholic University of Portugal, Faculty of Engineering, 2635-631 Rio de Mouro, Sintra, Portugal

<sup>d</sup>CEMEX, Faculty of Science and Technology, University of Coimbra, P-3004-516 Coimbra, Portugal

---

### Abstract

This paper presents the results of an experimental investigation to determine the effects of cryogenic coolant on surface integrity in orthogonal machining of hardened AISI 52100 bearing steel. Experiments were performed under dry and cryogenic conditions using chamfered CBN tool inserts. Several experimental techniques were used in the analyzing of the machined surface and subsurface: optical and scanning electron microscopes (SEM) were utilized for the surface topography characterization; chemical characterization (phase study) was carried out by means of Energy-dispersive spectroscopy (EDS) techniques; and X-ray diffraction (XRD) technique was used to determine residual stresses and phase changes induced by dry and cryogenic machining. The results show the benefits and the future potential of cryogenic cooling for surface integrity enhancement to achieve improved product's functional performance in hard machining.

© 2012 Published by Elsevier Ltd. Open access under [CC BY-NC-ND license](https://creativecommons.org/licenses/by-nc-nd/4.0/).

Selection and peer-review under responsibility of Prof. E. Brinksmeier

*Keywords:* Cutting, Surface integrity, Cryogenic cooling.

---

### 1. Introduction

Metal cutting processes are associated with high temperatures at the tool-chip and tool-workpiece interfaces, and the thermal aspects, in conjunction with the plastic deformation strongly affects the

---

\* Corresponding author. Tel.: +39-0984-494820; fax: +39-0984-494673.

E-mail address: [d.umbrello@unical.it](mailto:d.umbrello@unical.it), [d.umbrello@uky.edu](mailto:d.umbrello@uky.edu).

surface integrity and the quality of the machined product. In fact, the deformation process is concentrated in a very small zone and the local high temperatures due to heat generation have important consequences on the workpiece; consequently some microstructural alteration, often called the white layer formation, is some times produced. Such an affected layer, typically a few tens of microns thickness, hard and brittle, is considered to be detrimental to the life of machined component, since it has a significant impact on the magnitude of the maximum residual stresses and on the location of its compressive peak [1].

Numerous studies have been conducted on the white layer analysis during machining of hardened steels [2-4] and some of these were carried out on investigating the mechanisms related to white layer formation [3, 4] showing that its formation is mainly due to the rapid heating and quenching which produce untempered martensitic structures. Thus, it was generally believed that to reduce or avoid the white layer formation and, consequently to improve the surface integrity, it is necessary to decrease the temperatures; this is mainly done with the application of coolants. Also, the convective cooling effect of cutting fluids on this affected layer has not yet been clarified. König et al [5] suggested suppression of white layers with coolants, Zurecki et al [4] showed that cryogenic nitrogen spray cooling of cutting tool and tool-work contact would limit the thickness of white layer, but others [6] indicated no such effect. Moreover, only in few studies the effect of cryogenic coolant on the residual stress profiles are reported [4].

Therefore, the objective of this paper is to investigate the effects of cryogenic coolant on both white layer formation and residual stresses evolution during hard machining of AISI 52100. Experiments were performed under dry and cryogenic coolant conditions using chamfered CBN tool inserts at varying cutting speeds. Several experimental techniques were used in order to analyze the machined surface and subsurface. In particular, optical and scanning electron microscopes (SEM) were utilized for the surface topography characterization, the chemical characterization was carried out by means of Energy-dispersive spectroscopy (EDS) technique, and X-ray diffraction (XRD) technique was used to determine residual stresses and phase changes induced by machining under dry and cryogenic cooling conditions.

## 2. Experiments

Experiments were conducted on a stiff high speed CNC lathe equipped with an ICEFLY™ cryogenic fluid delivery system provided by Air Product Inc. (Fig. 1 a). In particular, orthogonal cutting operation was performed by using low CBN content cubic boron nitride tools (Seco grade: CBN 100) with chamfered geometry (ISO TNGN 110308S with a chamfer of 20°x0.1 mm) mounted on a CTFNR3225P11 tool holder (providing rake and clearance angles of -8° and 8°, respectively). The cryogenic coolant was applied by a nozzle to the area of interest indicated in Figure 1 (b) to provide the cooling effect at the primary, secondary and tertiary shear zones. Disks of hardened AISI 52100 steel (outer diameter = 150 mm, thickness = 1.4 mm) were prepared, machined and heat-treated.

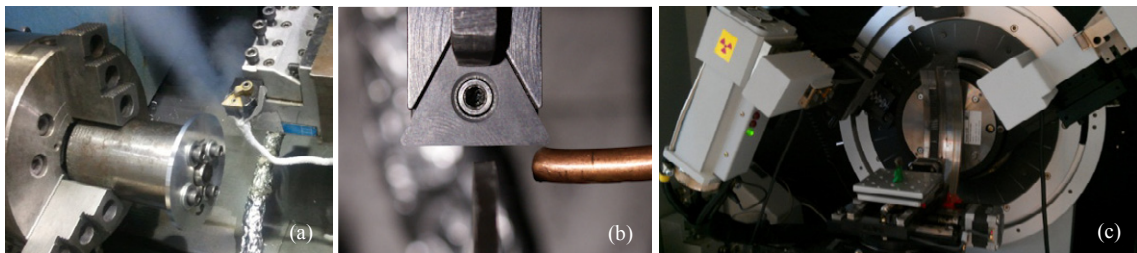


Fig. 1. (a) Experimental set-up for orthogonal cutting tests with cryogenic coolant system; (b) nozzle position for cryogenic coolant delivery; (c) X-ray equipment for microstructural phase composition analysis.

Heat treatments were performed in order to through-harden the disks to  $61\pm 1\text{HRC}$ . Then, disks were machined at varying cutting speeds (75 m/min, 150 m/min and 250 m/min) at a fixed feed rate of 0.075 mm/rev both for dry and cryogenic conditions; the cutting time of each test was 18-20 sec in order to reach the mechanical and thermal steady state conditions. In such conditions a flank wear of 0.03 – 0.05 mm was measured on the utilized CBN tools. Due to this smallness, the influence of tool wear was not investigated. After machining, samples of 5x5 mm were sectioned by wire-EDM for microstructure analysis and microhardness measurements. Then, the samples were polished and etched for about 5 s using 5% Nital solution to observe white layer using a light optical microscope (1000X) and a scanning electron microscope (SEM). By using the latter, it was also possible to execute an energy-dispersive X-ray spectroscopy (EDS) in order to conduct a qualitative elemental analysis of the machined surface.

Finally, a X-ray diffraction (XRD) Bruker AXS D8 Discover with a quarter Ellurian cradle sample holder was used in the investigation of the the microstructural phase composition of the machined material. The X-ray diffraction patterns were measured using  $\text{CuK}\alpha$  radiation ( $\lambda=1.54184\text{\AA}$ ,  $K_{\alpha 1}/K_{\alpha 2}=0.5$ ) from a source operated at 40 kV, and 40 mA. Samples were accordingly positioned at the center of plate into the X-ray goniometric in order to ensure a correct beam irradiation (Fig. 1 (c)). The  $2\theta$  scans were carried out between 40 and 54 deg  $2\theta$ . The scan increment was 0.02 degree; the corresponding acquisition time was accordingly varied. On the contrary, the residual stress state in machined disk surfaces was still analyzed by the XRD technique, but the  $\sin^2\psi$  method [7] was used (operating parameters are shown in Table 1). To determine the in-depth residual stress profiles, successive layers of material were removed by electropolishing to avoid the modification of machining-induced residual stress. Further corrections to the residual stress data were made due to the volume of material removed.

Table 1. X-Ray diffraction parameters for residual stress measurement

X-Ray radiation	Young's modulus	Poisson ratio	Bragg angle $2\theta$	Lattice plane	Number of $\psi$ angles ( $\pm 40^\circ$ )
Cr-K $\alpha$	210 GPa	0.3	156.3°	{2 1 1}	15

### 3. Results and discussion

#### 3.1. White layer and surface microhardness

Figure 2 (a) shows the experimental white layer thickness produced by varying the cutting speed and the cooling condition. In particular, the white layer ranges from less than 1  $\mu\text{m}$ , when using cryogenic conditions, to more than 7  $\mu\text{m}$  during dry cutting. Furthermore, the white layer increases with the increasing cutting speed. However, what is new is that the white layer depth obtained using cryogenic cooling is much smaller than the white layer thickness measured when dry machining was performed.

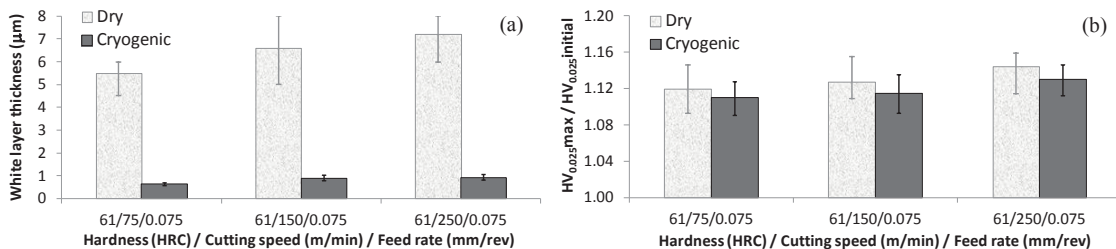


Fig. 2. (a) Experimental white layer thickness and (b) surface hardness modification at varying cutting speeds and the cooling methods (61 HRC and 0.075 mm/rev).

This significant difference was also observed in other investigation [8] and it is in agreement with the experimental results by Zurecki et al [4]. Figure 2 (b) shows the variation in microhardness values for the different experimental conditions employed. In particular, the results highlight that, in all of the investigated cases, the surface hardness is higher than that of the bulk material. Moreover, the value of the ratio  $HV_{0.025max}/HV_{0.025initial}$  decreases when lower cutting speed and cryogenic cooling were used.

### 3.2. Microstructural phase composition analysis

Figure 3 shows the phase analysis obtained by means of X-ray diffraction technique on both samples (machined under dry and cryogenic cooling conditions) and compares samples before the machining operation and, therefore, without the presence of the white layer on the investigated surface, and after machining with a white layer. In particular, the X-ray phase analysis on the unmachined surface shows only one peak at  $44.67^\circ$  which, according to Bragg's law and data reported in materials handbook [9], corresponds to ferrite- $\alpha$  at (110) Miller's indices. In contrast, when samples machined under dry condition were investigated, the X-ray phase analysis shows several peaks (Fig. 3 (a)). Once again, one peak is located at  $44.67^\circ$ , which corresponds to ferrite- $\alpha$ . Also, two additional peaks are found at  $43.74^\circ$  and  $50.67^\circ$ . Specifically, the peak at  $43.74^\circ$  in Figure 3 (a) corresponds to  $Fe_3C$ -martensite (102) while the peak at  $50.67^\circ$  corresponds to retained austenite at (200) Miller's indices as reported in materials handbook [9] and found by using Bragg's law.

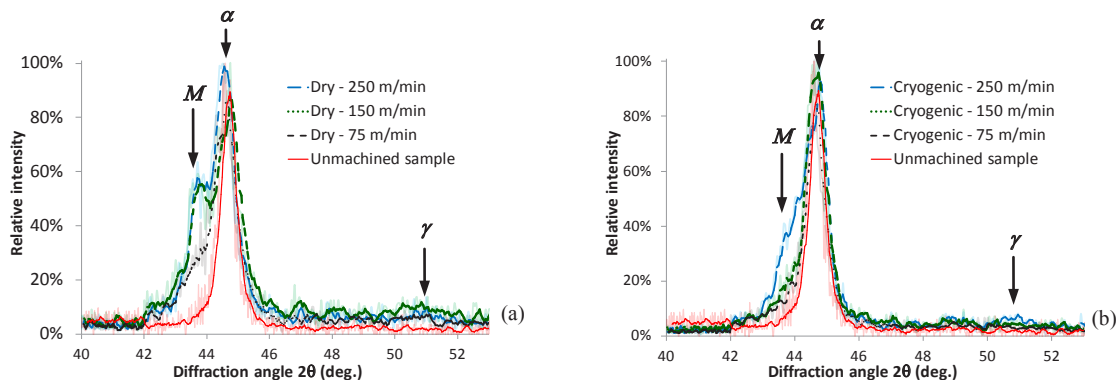


Fig. 3. X-ray phase analysis on specimens machined in dry conditions (a) and those machined with cryogenic cooling (b) vs. unmachined samples: 61 HRC, chamfered tool and 0.0.075 mm/rev ( $\alpha$  = ferrite- $\alpha$ ;  $\gamma$  = austenite; M =  $Fe_3C$ -martensite).

In contrast, the X-ray phase analysis conducted on sample machined under cryogenic cooling (Fig. 3 (b)) still shows the peaks referred to as ferrite- $\alpha$ , whereas the peak related to  $Fe_3C$ -martensite shows a significantly lower relative intensity (especially at 75 and 150 m/min). The peaks referred to the austenite are slightly higher (at 250 m/min) or similar (at 75 and 150 m/min) to those detected on the unmachined samples (Fig. 3 b). As the white layer was due to rapid heating and quenching (formation on untempered martensite structure), this experimental evidence shows that this layer is drastically reduced when hard machining is carried out with cryogenic cooling, i.e., less microstructural transformation due to rapid heating and quenching. This reduction of untempered martensite structure is also confirmed by energy-dispersive spectroscopy (EDS) analysis as depicted in Figure 4 (a). In particular, a higher carbon content in the surfaces of both machined specimens produced under different cooling conditions are detected, although the cryogenically machined surface presents a lower carbon content, i.e., less untempered martensite and retained austenite due to rapid heating and quenching.

### 3.3. Residual stress analysis

In this paragraph the influence of cutting speed, microstructural changes and cooling condition on the residual stresses are shown. To better describe their influence three different factors were considered (Fig. 4 (b)): *a*: Surface residual stress; *b*: Maximum compressive residual stress below surface and *c*: Penetration depth. Figure 5 (a) reports the values of both *a* and *b* parameters along the axial direction for all investigated cases in this research. The results show that both in dry and cryogenic machining *a* and *b* parameters are always compressive and they becomes thicker (i.e., deeper profile) as cutting speed increases, although those measured on samples machined under cryogenic cooling present smaller values than *a* and *b* observed in dry condition; furthermore, their rise is much smaller than that observed in dry condition. Similar trends are also noted along the hoop direction (Fig. 5 (b)). The reason for the higher compressive values for *a* and *b* parameters in dry machining can be attributed to the higher hardness values observed on the machined surface and below it. In fact, it was also demonstrated that residual stresses become more compressive with increasing hardness [10].

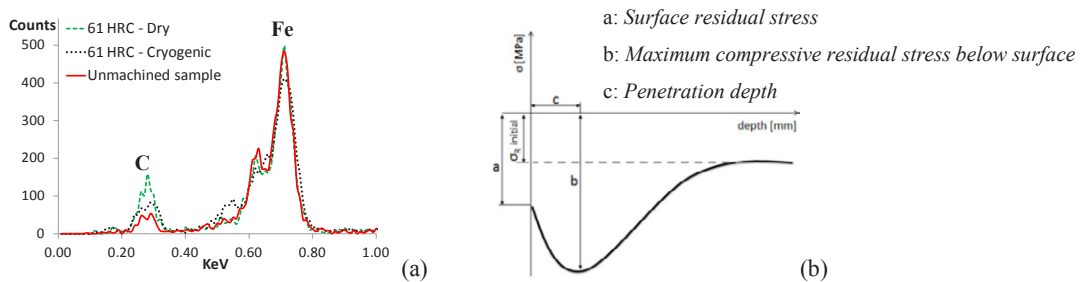


Fig. 4. (a) Energy-dispersive spectroscopy (EDS) analysis on specimens machined in dry and cryogenic cooling conditions vs. unmachined sample: 61 HRC, chamfered tool, 250 m/min and 0.125 mm/rev. (b) Residual stress parameters.

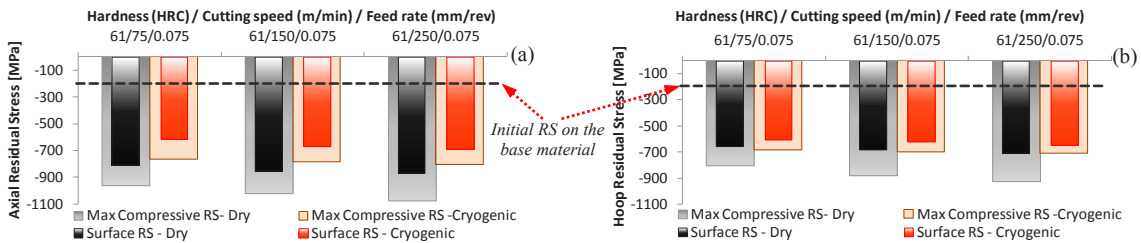


Fig. 5. Surface and maximum compressive residual stresses along the axial (a) hoop (b) directions at varying cutting speeds and cooling methods (61 HRC and 0.075 mm/rev).

Another factor of immense interest, related to the residual stress profile, is the penetration depth (i.e., location of maximum compressive residual stress). In fact, it is known that the white layer is likely to impair the fatigue life of the part in the case of hardened steels and, as a consequence, is usually removed before the use of the component. Therefore, it is important to investigate where the maximum compressive residual stress is located. As observed in Figures 6 (a) and (b), when machining is carried out in dry condition, the penetration depth both for axial and hoop directions is positioned into the white layer or, for the highest used cutting speed, only a fraction of a micron deeper. Such evidence is detrimental to the fatigue life of any machined components since, even in the case of gently removing of the white layer thickness (in a manner which does not modify the machining-induced residual stress profile), most of the compressive area [1] will be lost. As a consequence, the fatigue life will be drastically reduced.

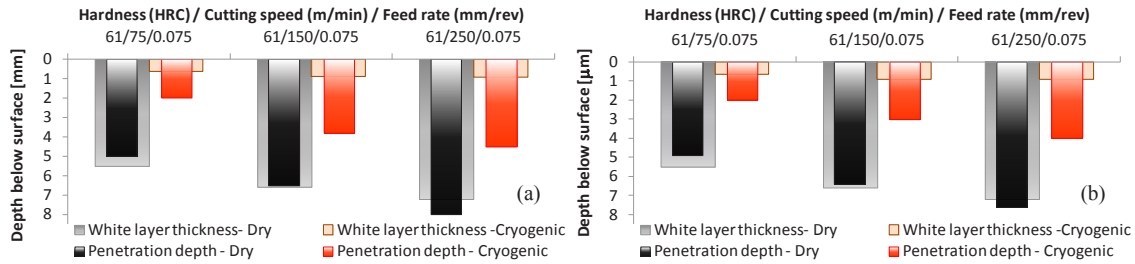


Fig. 6. Penetration depth vs. white layer thickness on both axial (a) hoop (b) directions at varying cutting speeds and cooling methods (61 HRC and 0.075 mm/rev).

In contrast, the application of cryogenic coolant permits one to achieve the benefit of having the penetration depth always at much higher and deeper than the white layer thickness (Figure 6) both for the axial and hoop directions. Therefore, the compressive area of components machined under cryogenic condition after the post removal operation can be higher than the one obtained in dry machining.

#### 4. Conclusions

Experimental observations reported in this study suggest that the use of cryogenic coolant in machining of hardened AISI 52100 significantly affects the white layer formation and the residual stresses. In particular, cryogenic cooling condition reduces the white layer thickness. In contrast, dry machining produces a thicker white layer which is detrimental for the product's performance and relative cost (secondary operation for removal is needed) and, although the compressive residual stresses are deeper, the position of the penetration depth into the white layer thickness impairs the fatigue life. Therefore, it can be concluded that the cryogenic cooling helps to enhance several aspects of the surface integrity of hard machined components.

#### References

- [1] Hashimoto F, Melkote SN, Singh R, Kalil R. Effect of Finishing Methods on Surface Characteristics and Performance of Precision Components in Rolling/Sliding Contact, *Int. J. Mach. & Machinability of Mater.* 2009; **6/1-2**: 3-15.
- [2] Ramesh A, Melkote SN, Allard LF, Riester L, Watkins, TR. Analysis of White Layers Formed in Hard Turning of AISI 52100 Steel, *Mater. Sci. & Eng. – A.* 2005; **390**: 88-97.
- [3] Barry J, Byrne G. TEM Study on the Surface White Layer in Two Turned Hardened Steels, *J. Mater. Sci. Eng. – A.* 2002; **25**: 356-364.
- [4] Zurecki Z, Ghosh R, Frey, JH. Investigation of White Layer Formed in Conventional and Cryogenic Hard Turning of Steels, *ASME International Mechanical Engineering Congress and Exposition, Washington.* 2003; 16-21.
- [5] König W, Klinger M, Link R. Machining Hard Materials with Geometrically Defined Cutting Edges – Field of Applications and Limitations, *Annals of the CIRP.* 1990; **57/1**: 61-64.
- [6] Tonshoff, HK, Brandt D, Wobker, HG. Potential and Limitation of Hard Turning, *1<sup>st</sup> Int. Machining and Grinding Conf., SME Technical Paper MR 95-215, Dearborn, Michigan.* 1995; 965-978.
- [7] Noyan IC, Cohen JB. Residual Stress-Measurement by Diffraction and Interpretation, *Springer*, New York.
- [8] Umbrello D, Caruso S, Di Renzo S, Jayal, AD, Dillon OW Jr., Jawahir IS. Dry vs. Cryogenic Orthogonal Hard Machining: an Experimental Investigation, *14<sup>th</sup> ESAFORM Conference, AIP Conference Proceedings.* 2011; **1353**: 627-632.
- [9] Joint Committee on Powder Diffraction Standards (JCPDS). Powder Diffraction File, *Inorganic Volume.* 1990; **Sets 6-36**.
- [10] Thiele JD, Melkote SN, Peascoe RA, Watkins TR. Effect of Cutting-Edge Geometry and Workpiece Hardness on Surface Residual Stresses in Finish Hard Turning of AISI 52100 Steel, *ASME J. Manuf. Sc. & Eng.*, 2000; **122**: 642-649